# **JAAS**



# **PAPER**

View Article Online
View Journal | View Issue



Cite this: *J. Anal. At. Spectrom.*, 2025, **40**, 1394

Received 22nd January 2025 Accepted 10th April 2025

DOI: 10.1039/d5ja00030k

rsc.li/jaas

# In situ Re-Os geochronology of Re-rich Palaeogene molybdenite by LA-ICP-MS/MS†

Stijn Glorie, 6 \*a Jay M. Thompson, 6 \*b Sarah E. Gilbert 6 \*c and A. Kate Souders 6 \*b

In situ Re–Os geochronology by LA-ICP-MS/MS was previously demonstrated by reacting Os with CH<sub>4</sub> or N<sub>2</sub>O reaction gasses. However, for both reactions, a minor proportion of the Re parent isotope also reacts, potentially leading to significant isobaric interferences of  $^{187}$ Re on  $^{187}$ Os, especially for young samples with little radiogenic in-growth. Here we present an interlaboratory comparison and compare three reaction gas mixtures (CH<sub>4</sub> + H<sub>2</sub> + He, N<sub>2</sub>O and N<sub>2</sub>O + He) with the aim to robustly date Palaeogene (66–23 Ma) molybdenite from the Bingham Canyon and Henderson deposits. CH<sub>4</sub> mixed with H<sub>2</sub> gas gives the highest sensitivity, while N<sub>2</sub>O and He gas buffer Re reaction. On balance, the analytical method involving N<sub>2</sub>O + He reaction gas is most suitable for dating Palaeogene molybdenite, resulting in age precision of 2.6% for Bingham and 5.8% for Henderson. For older, >1 Ga molybdenite, CH<sub>4</sub> + H<sub>2</sub> + He may give comparatively better age precision.

# Introduction

Molybdenite Re-Os geochronology is widely used in ore and hydrocarbon exploration (e.g. ref. 1 and 2). The conventional analytical approach involves isotope dilution followed by isotope ratio measurements with a Thermal Ionization Mass Spectrometer (TIMS), which is a laborious and timeconsuming method that is conducted at highly specialized laboratories.3,4 Recent developments in reaction gas massspectrometry now allow Re and Os isotopes to be rapidly measured in situ using laser ablation inductively coupled plasma tandem mass-spectrometry (LA-ICP-MS/MS) at high spatial resolution.5-7 Hogmalm et al.5 and Tamblyn et al.6 demonstrated that Os efficiently reacts with CH4 to form OsCH<sub>2</sub><sup>+</sup>, inducing a +14 amu mass-shift. This reaction occurs at a much higher rate (ca. 120 $\times$ ) compared to isobaric ReCH<sub>2</sub><sup>+</sup> production. However, the ca. 1-2% Re reaction accounts for potentially significant interference on mass 201 amu (187Os12C1H2, referred here as 187+14Os), especially for young samples with relatively low 187Os ingrowth. More recently, Simpson et al. showed that Os reacts with N<sub>2</sub>O to form OsO<sub>4</sub>, inducing a +64 amu mass-shift for 187Os 16O4 (referred here as  $^{187+64}$ Os). The equivalent reaction of Re can be reduced to ca. 0.15%, which is about an order of magnitude lower than for the CH<sub>4</sub> method.<sup>6</sup> However, while the interference correction is larger, generally, higher sensitivity (count rates) can be achieved with the  $CH_4$  method. The obtainable precision on the resulting Re–Os date is a balance between (1) increasing sensitivity and better counting statistics, and (2) reducing the interference correction, which also reduces count rates. Here we explore the limitations of the LA-ICP-MS/MS method on Cenozoic (<66 Ma) samples, with both the  $N_2O$  and  $CH_4$  reaction gas methods. In addition to published reaction gas methodologies, we also explore the effects of mixing reaction gasses by adding  $H_2$  and/or He to  $CH_4$  or  $N_2O$  in the reaction cell. We further present the first interlaboratory comparison for the *in situ* Re–Os molybdenite dating method.

# Sample descriptions

#### Bingham Canyon molybdenite

Molybdenite was sampled from the high-grade ore zone of the Bingham Canyon porphyry deposit in northern Utah, United States (US). This sample is a porphyritic intrusive that contains the following minerals: quartz (45%, 2 to 10 mm), altered feldspar (40%, 2 to 5 mm), biotite ( $\sim$ 2%, 0.2 to 0.5 mm), chalcopyrite ( $\sim$ 1%, <0.2 mm) and molybdenite ( $\sim$ 12%, 0.5 to >5 mm). Molybdenite occurs as aggregates and veins up to 10 mm in size of several millimetre-sized individual molybdenite crystals. The selected molybdenite grains were 0.5 to 2 mm in size and separated from the whole rock sample by gentle crushing and picking of grains onto double-sided tape prior to mounting in epoxy resin. The sample was then polished using fine SiC sandpaper (1000 and 2000 grit), finished using 1 μm suspended diamond paste and cleaned with ethanol. The age of the molybdenite from this deposit is dated by conventional N-TIMS Re-Os at 37.0  $\pm$  0.27 Ma.8 The reported uncertainty is 2 SEM (=2 standard error of the mean).

<sup>&</sup>lt;sup>a</sup>Dept. of Earth Sciences, University of Adelaide, Adelaide, SA 5005, Australia. E-mail: stijn.glorie@adelaide.edu.au

<sup>&</sup>lt;sup>b</sup>U.S. Geological Survey, Denver, CO 80225, USA

<sup>&#</sup>x27;Adelaide Microscopy, University of Adelaide, Adelaide, SA 5005, Australia

 $<sup>\</sup>dagger$  Electronic supplementary information (ESI) available. See DOI: https://doi.org/10.1039/d5ja00030k

Paper JAAS

#### Henderson mine/RM 8599

Molybdenite was sampled from the high-grade ore concentrate in the Henderson mine, Colorado, US. This sample was measured as individual molybdenite grains from the original porphyritic rock sample as well as the mechanically homogenized RM 8599 powder purchased from the National Institute of Standards and Technology (NIST). The molybdenite grains from the whole rock sample were 0.5 to 2 mm in size and separated from the rock matrix by gentle crushing and picking of grains onto double-sided tape prior to mounting in epoxy resin. The sample was then polished using fine SiC sandpaper (1000 and 2000 grit), finished using 1 µm suspended diamond paste and cleaned with ethanol. The RM 8599 powder was prepared by pressing ~2 grams into a 11 mm pellet at 10 tons of pressure (30 second holding time). The conventional N-TIMS Re-Os reference age of the RM 8599 sample is  $27.656 \pm 0.022$  Ma. The individual molybdenite grains are assumed to be the same age as this molybdenite powder.

#### **Analytical methods**

The molybdenite samples were analysed at the United States Geological Survey (USGS) Denver Federal Centre (Geology, Geophysics, and Geochemistry Science Center), Colorado, US and Adelaide Microscopy, University of Adelaide, Australia, for laboratory comparison purposes.

#### US geological survey

At the USGS the analyses were performed in the USGS-LTRACE laboratory. A total of 6 analytical sessions are reported. Analyses from 2021 and 2022 were conducted using a Photon Machines Analyte G2 laser system with an ATL ArF excimer source operating at 193 nm wavelength and  $\sim\!5$  n pulse width. Analyses from 2023 onward were conducted using a RESOlution-SE 193 nm laser ablation system also with an ATL excimer laser source. Both laser systems were coupled to an Agilent 8900x ICP-MS/MS. The laser fluence was varied between 3.5 and 6 J cm $^{-2}$ , depending on the session, spot size was between 80 and 120 microns, and laser repetition rate was between 10 and 20 Hz. All analyses were performed in a helium atmosphere and signal smoothing of laser pulses was achieved using the 'squid' signal smoother. Nitrogen (N2) was added to the Ar carrier gas before the ICP-MS to increase sensitivity.

The ICP-MS tuning was first performed in single-quad mode for maximum heavy mass sensitivity while achieving a ThO/Th rate of <0.2% and U/Th <1.1 for the S-155 ablation cell and  $\sim$ 1.2 for the HelEx cell (Analyte G2). Tuning was performed using the NIST612 glass with a  $\sim$ 40 micron square beam (38 micron beam for the RESOlution-SE system), 10 Hz, 3.5 J cm<sup>-2</sup> and 3 microns per s line scan speed. Under these conditions, the count rate for  $^{238}$ U was  $\sim$ 1 Mcps. Once optimized in single-quad mode, the instrument was set to MS/MS mode with reaction gases CH<sub>4</sub> (6% or 0.07 ml min<sup>-1</sup>), He (4.8 to 6.3 ml min<sup>-1</sup>) and H<sub>2</sub> (5.0 to 5.4 ml min<sup>-1</sup>). See ESI 1† <sup>10</sup> for further ICP-MS/MS setting details. The  $^{185}$ Re  $^{12}$ CH<sub>2</sub>/ $^{185}$ Re ratio was monitored during tuning and reaction gas flow rates and octupole settings were adjusted to minimize this ratio ( $\sim$ 0.3 to  $\sim$ 0.4) while still maintaining

sensitivity for the <sup>185</sup>Re signal. The MASS-3 FeS pressed powder from the USGS was used for monitoring Os signal, but tuning specifically for Os was not feasible due to heterogeneities in the Os content of this material (5 to 10% variation). The isotopes measured during analysis vary between sessions (ESI 1†).<sup>10</sup> Isotopes measured in each session (with dwell times in milliseconds in parenthesis) are: <sup>57</sup>Fe (2), <sup>185</sup>Re (20), <sup>185+14</sup>Re (50–80), <sup>187</sup>Os (20), <sup>187+14</sup>Os (200), <sup>188+14</sup>Os (200).

The correction for reacted Re with the CH<sub>4</sub> gas was calculated using Os-free NIST612 glass using the mass shifted Re at masses 199 (185Re<sup>12</sup>CH<sub>2</sub>) and 201 (187Re<sup>12</sup>CH<sub>2</sub>) and the methodology presented in ref. 5 and 6 assuming natural Re abundances ( $^{185}$ Re/ $^{187}$ Re = 0.59738 ± 0.00039 (ref. 11)). Subsequently, an in-house Moly Hill molybdenite was used to calibrate the Re/Os ratio of the Henderson and Bingham molybdenites assuming an age of 2680  $\pm$  90 Ma ( $^{187}$ Os/ $^{187}$ Re =  $0.04566 \pm 0.00153$ ). 12 Note that this is a different piece of Moly Hill molybdenite to the reference material characterised in ref. 6 188Os/187Os ratios are not reported for the USGS data as all <sup>189</sup>Os data (used as a proxy for <sup>188</sup>Os) were effectively below detection limit. Data reduction, involving background subtraction, interference, drift corrections, and ratio normalisation, were conducted using the LADR software v. 1.1.7.13 Given interference subtracted count rates on 187+14Os in the timeresolved signals fall occasionally below zero, LADR fails to accurately calculate the signal precision uncertainty on the corrected 185Re/187+14Os ratios. Hence, signal precision uncertainties were calculated manually using spreadsheets by setting negative values to zero prior to calculating the standard deviation on the 187+14Os signal. All other sources of uncertainty (Table 1) are subsequently propagated to the calculated signal precision uncertainties. Reported fully propagated uncertainties on the isotope ratios are 2 SEM. No correction for downhole Re-Os fractionation was made.6 Age calculations were conducted as weighted means in IsoplotR from the corrected <sup>187</sup>Os/<sup>187</sup>Re ratios<sup>14</sup> and age uncertainties are reported as 95% confidence uncertainties.

## Adelaide microscopy

At Adelaide microscopy, Re–Os isotope analysis was conducted on a RESOlution-SE 193 nm laser ablation system coupled to an Agilent 8900× ICP-MS/MS over two analytical sessions. The molybdenites were sampled by static spot ablation at 3 J cm $^{-2}$  and the aerosol was transported to the plasma in a gas atmosphere of 1 l min $^{-1}$  Ar, 0.38 l min $^{-1}$  He and 4 ml min $^{-1}$  N<sub>2</sub>. Given the absence of Re–Os down-hole fractionation,6 laser beam diameters and repetition rates were variable (30–100  $\mu$ m, 7–10 Hz) between reference materials and samples, with the aim to maximize count rates while keeping Re count rates under the pulse/analog threshold for the detector (see ESI 1† for details).

For each session, the mass-spectrometer was first tuned in absence of reaction gas to demonstrate a robust plasma (*e.g.* ThO/Th rate of <0.2% and U/Th <1.1). Subsequently, for session 1, a mixture of  $CH_4$  (0.22 ml min<sup>-1</sup>) + He (5 ml min<sup>-1</sup>) +  $H_2$  (6 ml min<sup>-1</sup>) was used in the reaction cell, tuned to maximise count rates.  $H_2$  was used to enhance sensitivity, while He was

**Table 1** Propagated uncertainties in the analytical workflow. S = session. 187 + X refers to the mass-shift on Os with X being 14 amu for CH<sub>4</sub> and 64 amu for N<sub>2</sub>O

	Adelaide			NSGS					
Systematic uncertainties	S1: 7/12/2023	S2a: 14/12/2023	S2b: 14/12/2023	S1: 17/11/2021	S2: 22/11/2021	S3: 23/11/2021	S4: 4/07/2022	S5: 29/9/2023	S6: 26/6/2024
Calibration curve missfit Re/ Os ratio	0.92%	%98.0	1.69%	1.39%	1.71%	0.61%	1.02%	0.74%	0.56%
Calibration curve missfit Os/ Os ratio	0.55%	0.62%	0.62%	0.34%	0.38%	0.51%	0.72%	0.04%	0.24%
Uncertainty in measured Re/ Os ratio for RM (Qmoly Hill)	0.11%	0.14%	0.24%	0.36%	0.25%	0.24%	0.50%	0.26%	0.24%
Uncertainty in measured Os/ Os ratio for RM (NiS3)	%60.0	0.14%	0.14%	0.23%	0.21%	0.20%	0.32%	0.16%	0.11%
Uncertainty in mass bias	0.04%	0.12%	0.11%	0.34%	0.37%	0.35%	0.24%	0.34%	0.14%
Long-term reproducibility of reference materials	Not propagated	Not propagated uncertainties (insufficient data)	ıfficient data)						
Random uncertainties									
Signal precision of interference corrected <sup>187+X</sup> Os Signal precision of <sup>185</sup> Re Signal precision of <sup>189+X</sup> Os Uncertainty in blank subtraction Uncertainty in interference correction factor (~signal precision of Added age uncertainty for overdispersion if present (IsoplotR)	e corrected <sup>187+X</sup> O on rrection factor (~s rdispersion if pres	gnal precision of	<sup>185+X</sup> Re)						

0.10%

(Qmoly Hill) Theoretical uncertainty in reference Os/Os ratio for RM

IDTIMS Re/Os ratio for RM Uncertainty in reference

Constants

0.51%

(NiS3) Uncertainty in decay constant

0.06%

(IsoplotR default) Uncertainty in initial Os/Os ratio anchor (IsoplotR default)

 Table 2
 Analytical results for reference materials and molybdenites from Bingham Canyon and Henderson<sup>a</sup>

Session	Reaction gas	$n^c$	<sup>185</sup> Re (cps)	±2SEM	185+xRe (cps)	±2SEM	$^{187+x}Os^b$ (cps)	±2SEM	$^{187+x}Os^b$ (cps)	$\pm 2 \mathrm{SEM}$	Interf. <sup>e</sup> (%)	fRe RR (%)	Age (Ma) <sup>g</sup>	±CI (Ma)	$\pm \text{CI}^h$ (%)	MSWD <sup>i</sup>
Adelaide							Measured		$\mathrm{Corrected}^d$							
QMolyHill 1 2a 2b	QMolyHill primary RM (IDTIMS: $2624 \pm 5 \text{ Ma}$ )  1 CH <sub>4</sub> + He + H <sub>2</sub> 30 545 008  2a N <sub>2</sub> O 16 462 690  2b N <sub>2</sub> O + He 6 518 434	30 30 16 6	524 ± 5 Ma) 545 008 462 690 518 434	58 015 97 879 95 257	3120 863 118	334 198 19	30 097 24 508 14 167	3184 5605 2783	24 746 23 023 13 968	2611 5265 2750	18% 6% 2%	0.57% 0.19% 0.02%	2625 2625 2624	9 28 12 29 38 46	1.1% 1.1% 1.8%	1.0 1.0 1.0
M252 secol 1 2a 2b	M252 secondary RM (IDTIMS: 1520 $\pm$ 4 Ma) 1 $CH_4 + He + H_2$ 30 790 180 2a $N_2O$ 16 1574 83 2b $N_2O + He$ 6 1953 41:	IS: 1520 30 16 6	1 4 Ma) 790 180 1 574 831 1 953 411	149 834 243 405 761 730	4463 2766 474	838 418 196	27 946 46 691 29 925	5283 7116 11 571	20 307 41 929 29 107	3848 6397 11 235	28% 10% 3%	0.56% 0.18% 0.02%	1505 1500 1514	6.5 16 11 20 23 28	1.1% 1.3% 1.8%	0.83 1.9 0.5
Bingham (l 1 2a 2b	$\begin{array}{llllllllllllllllllllllllllllllllllll$	28 18 18 18	879 007 724 950 711 728	64 792 33 786 38 923	5150 1193 157	379 58 9	9499 2495 542	701 121 29	683 443 272	168 68 30	93% 83% 49%	0.59% 0.16% 0.02%	45.4 36.5 37.9	1.9 2.0 1.3 1.3 0.9 1.0	4.4% 3.6% 2.6%	0.62 0.52 0.35
Henderson 1 2a 2b	Henderson (IDTIMS: 27.656 $\pm$ 0.022 Ma) 1 $CH_4 + He + H_2$ 26 200 2a $N_2O$ 18 117 2b $N_2O + He$ 96	0.025 $0.025$ $0.025$ $0.025$ $0.025$ $0.025$	2 Ma) 200 280 117 332 96 570	27 584 11 678 8575	1185 188 23	162 19 2	2151 375 66	296 39 6	121 50 26	38 14 7	95% 87% 58%	0.59% 0.16% 0.02%	30.9 23.3 27.5	3.9 3.9 3.1 3.1 1.6 1.6	13% 13% 5.8%	3.7 3.3 1.6
Session	Reaction gas		(cps)	±2SEM	(cps)	±2SEM	$\frac{^{187+x}Os^b}{(cps)}$ Measured	±2SEM	$\frac{^{187+x}Os^b}{(cps)}$ Corrected <sup>c</sup>	$\pm 2SEM$	Interf. <sup>d</sup> (%)	Re RR <sup>e</sup>	Age <sup>f</sup> (Ma)	$\pm \mathrm{CI}^g$ (Ma)	$\pm \mathrm{CI}^g$	$\overline{\text{MSWD}^h}$
Moly Hill F 1 2 3 3 4 4 6	Moly Hill primary RM (IDTIMS: $2680 \pm 90$ Ma)  1 CH <sub>4</sub> + He + H <sub>2</sub> 9 866 292  2 CH <sub>4</sub> + He + H <sub>2</sub> 11 2 046 608  3 CH <sub>4</sub> + He + H <sub>2</sub> 10 133 768  4 CH <sub>4</sub> + He + H <sub>2</sub> 12 1167 149  5 CH <sub>4</sub> + He + H <sub>2</sub> 14 644 773  6 CH <sub>4</sub> + He + H <sub>2</sub> 19 466 349	MS: 268 9 11 2 10 1 12 1 14 14		213 714 357 149 251 245 191 059 127 330 62 345	2719 6674 4248 12 850 2605 1927	669 11141 803 2580 521 255	36 328 93 533 60 408 65 312 42 428 30 604	9056 16 383 11 493 12 677 8206 3972	31 705 82 195 53 172 43 514 38 015 27 306	7916 14 448 10 124 8495 7334 3539	13% 12% 16% 33% 10%	0.31% 0.33% 0.32% 1.10% 0.40%	2687 2689 2687 2689 2690 2690	28 36 28 38 12 29 24 36 12 29 27 27	1.3% 1.4% 1.1% 1.3% 1.1%	11 0.7 1.6 0.7 0.7
Bingham (1 1 2 3 4 4 5 6	Bingham (IDTIMS: $37.0 \pm 0.27$ Ma)  1 $CH_4 + He + H_2                                  $	1.27 Ma) 5 1 6 1 5 1 10 16	1063 763 1359 430 2449 963 1756 781 880 153 450 317	241 044 106 220 461 924 283 965 88 079 48 575	3379 4678 7805 18 551 3518 1809	778 359 1456 3035 358 198	6256 8729 14 820 32 826 7010 3459	1425 658 2771 5334 629 384	500 772 1545 1352 777 372	152 201 333 423 265 175	92% 91% 90% 86% 88%	0.32% 0.34% 0.32% 1.06% 0.40%	36.1 39.5 42.9 36.9 40.0	4.8   4.8   4.1   4.1   4.1   4.1   4.0   4.0   4.0   3.5   5.2   5.2	13% 10% 9.6% 11% 8.8%	0.6 0.9 0.04 0.9 2.6

Table 2 (Contd.)

930     44     1701     95     116     37     93%     0.32%     25.5     5.9 5.9     23%       434     91     794     164     59     20     93%     0.34%     29.4     9.1 9.1     31%       4537     115     8002     196     288     109     96%     1.00%     22.1     6.7 6.7     30%       380     62     714     120     60     22     91%     0.41%     20.1     5.6 5.6     28%       644     135     1205     253     93     40     90%     0.40%     26.1     3.3 3.3     13%	Session	Reaction gas		<sup>185</sup> Re (cps)	$\pm 2 \mathrm{SEM}$	<sup>185+x</sup> Re (cps)	±2SEM	$^{187+x}\mathrm{Os}^{b}$ (cps)	$\pm 2 \mathrm{SEM}$	$^{187+x}\mathrm{Os}^{b}$ (cps)	$\pm 2 \mathrm{SEM}$	Interf. <sup>d</sup> (%)	${\rm Re}\ {\rm RR}^e \\ (\%)$	$Age^f$ (Ma)	$\pm  ext{CI}^g$ (Ma)	$\pm \text{CI}^g$ (%)	$\mathrm{MSWD}^h$
26         15 817         930         44         1701         95         116         37         93%         0.32%         25.5         5.9   5.9         23%           0.4         26 237         434         91         794         164         59         20         93%         0.34%         29.4         9.1   9.1         31%           0.3         10 291         1497         34         2759         58         216         56         93%         0.32%         29.3         4.5   4.5         15%           3.8         11020         4537         115         8002         196         288         109         96%         1.00%         22.1         6.7   6.7         30%           84         15 293         380         62         714         120         60         22         91%         0.41%         20.1         5.6   5.6         28%           48         34 540         644         135         1205         253         93         40         90%         0.40%         26.1         3.3   3.3         13%	USGS		l					Measured	ı	$Corrected^c$	ı						
26         15 817         930         44         1701         95         116         37         93%         0.32%         5.9         5.9         23%           04         26 237         434         91         794         164         59         20         93%         0.34%         59.4         9.1 9.1         31%           03         10 291         1497         34         2759         58         216         56         93%         0.32%         29.3         4.5 4.5         15%           38         11 020         4537         115         8002         196         288         109         96%         1.00%         22.1         6.7 6.7         30%           44         15 293         380         62         714         120         60         22         91%         0.41%         20.1         5.6 5.6         28%           48         34 540         644         135         1205         253         93         40         90%         0.40%         26.1         3.3 3.3         13%	Hender	son (IDTIMS: 27.656	5 ± 0.02	22 Ma)													
6         126 604         26 237         434         91         794         164         59         20         93%         0.34%         29.4         9.1 9.1         31%           8         463 603         10 291         1497         34         2759         58         216         56         93%         0.32%         29.3         4.5 4.5         15%           14         453 338         11 020         4537         115         8002         196         288         109         96%         1.00%         22.1         6.7 6.7         30%           11         93 184         15 293         380         62         714         120         60         22         91%         0.41%         20.1         5.6 5.6         28%           17         161 548         34 540         644         135         1205         253         93         40         90%         0.40%         26.1         3.3 3.3         13%	1	$CH_4$ + He + $H_2$	∞	292,726	15 817	930	44	1701	95	116	37	93%	0.32%	25.5	5.9 5.9	23%	2.8
8         463 603         10 291         1497         34         2759         58         216         56         93%         0.32%         29.3         4.5  4.5         15%         15%           14         453 338         11 020         4537         115         8002         196         288         109         96%         1.00%         22.1         6.7   6.7         30%           11         93 184         15 293         380         62         714         120         60         22         91%         0.41%         20.1         5.6   5.6         28%           17         161 548         34 540         644         135         1205         253         93         40         90%         0.40%         26.1         3.3   3.3         13%	2	$CH_4$ + He + $H_2$	9	126604	26 237	434	91	794	164	59	20	93%	0.34%	29.4	9.1 9.1	31%	4.6
14     453 338     11 020     453 338     11 020     453 338     11 020     453 338     10 020     10 041%     1	3	$CH_4$ + $He$ + $H_2$	8	463 603	10291	1497	34	2759	28	216	26	93%	0.32%	29.3	4.5 4.5	15%	2.8
11         93184         15 293         380         62         714         120         60         22         91%         0.41%         20.1         5.6 5.6         28%           17         161548         34540         644         135         1205         253         93         40         90%         0.40%         26.1         3.3 3.3         13%	4	$CH_4 + He + H_2$	14	453 338	11020	4537	115	8002	196	288	109	<b>%96</b>	1.00%	22.1	6.7   6.7	30%	6.9
$17  161548  34540  644  135  1205  253  93  40  90\%  0.40\%  26.1  3.3 \\   3.3  13\%  13$	5	$CH_4$ + He + $H_2$	11	93 184	15 293	380	62	714	120	09	22	91%	0.41%	20.1	5.6 5.6	28%	5.4
	9	$CH_4 + He + H_2$	17	161 548	34 540	644	135	1205	253	93	40	%06	0.40%	26.1	3.3 3.3	13%	1.7

 $^2$  All cps (=counts per second) values are back-ground substracted.  $^b$   $_x = 14$  amu for CH $_4$  reaction to OsCH $_2^+$ , = 64 amu for N $_2$ O reaction to OsO $_4^+$ .  $^c$   $_n =$  Number of analyses per sample.  $^d$  Corrected refers to the interference correction of  $^{187+8}$ Re on  $^{187+8}$ Re on  $^{187+8}$ Re on 187+8 by cps subtraction.  $^c$  Interf. is the percentage interference of  $^{187+8}$ Re on  $^{187+8}$ Re is the Re reaction rate calculated as the ratio of 185+xRe on 185Re. g Age is the calculated weighted mean Re-Os age in IsoplotR. h ±CI is the 95% confidence interval uncertainty on the age, calculated using added uncertainty for over dispersion = Mean squared weighted reported for the maximum propagated uncertainty. ' MSWD where required. The second number also includes the uncertainty on the decay constant. % deviation. used to buffer  $^{187}\text{Re}^{12}\text{CH}_2$  interference production. In the second session,  $N_2\text{O}$  (0.32 ml min $^{-1}$ ) was used as the reaction gas, first (session 2a) without added He (maximum sensitivity) and secondly (session 2b) with added He (5 ml min $^{-1}$ ) to reduce the interference. Lense parameters and reaction cell settings were similar between both methods, detailed in ESI 1.† The isotopes measured during analysis vary between sessions (ESI 1†). Isotopes measured in each session (with dwell times in milliseconds in parenthesis) are:  $^{95}\text{Mo}$  (2),  $^{185}\text{Re}$  (20),  $^{185+X}\text{Re}$  (50–100),  $^{187}\text{Os}$  (50),  $^{187+X}\text{Os}$  (100),  $^{189}\text{Os}$  (50),  $^{189+X}\text{Os}$  (100–200).

The measured  $^{185}$ Re/ $^{187+\hat{x}}$ Os ratios (with x=14 amu for CH<sub>4</sub> method, x = 64 amu for N<sub>2</sub>O method) were corrected for  $^{187+x}$ Re interference on <sup>187+x</sup>Os, taking into account the mass-bias on the <sup>187</sup>Re/<sup>185</sup>Re ratio, measured in Os-free NIST610 glass (see details in ESI 1†), and subsequently calibrated to the QMolyHill reference molybdenite (N-TIMS  $^{187}$ Os/ $^{187}$ Re ratio = 0.044699  $\pm$ 0.000166, age =  $2624 \pm 5$  Ma, 2SEM uncertainties<sup>6</sup>). The <sup>188</sup>Os/<sup>187</sup>Os ratios were calibrated using NiS-3, <sup>15</sup> using measured <sup>189+X</sup>Os as a proxy for <sup>188</sup>Os and assuming a present-day  $^{188}$ Os/ $^{187}$ Os ratio of 6.740  $\pm$  0.004. $^{16}$  Data reduction, involving background subtraction, interference, drift corrections, and ratio normalisation, were conducted using the LADR software v. 1.1.7.13 As above, signal precision uncertainties were calculated manually using a script by setting negative values to zero prior to calculating the standard deviation on the <sup>187+14</sup>Os signal. All other sources of uncertainty (Table 1) are subsequently propagated to the calculated signal precision uncertainties. Reported fully propagated uncertainties on the isotope ratios are 2 SEM. Age calculations were conducted as weighted means in IsoplotR from the corrected 187Os/187Re ratios14 and age uncertainties are reported as 95% confidence uncertainties.

Reference molybdenite M252 from the Merlin deposit (Queensland, Australia) was used as secondary reference material to verify accuracy in isotope ratio determinations (N-TIMS  $^{187}\text{Os}/^{187}\text{Re}$  ratio = 0.025649  $\pm$  0.000105, age = 1520  $\pm$  4 Ma (ref. 6)). The obtained Re–Os dates are 1505  $\pm$  16 Ma (session 1), 1500  $\pm$  20 Ma (session 2a) and 1514  $\pm$  28 Ma (session 2b), in agreement with the reference age. Isotopic ratio uncertainties and age uncertainties are quoted as 2 standard error of the mean.

# Results

#### Sensitivity and interferences

For the USGS sessions (all with  $CH_4 + H_2 + He$  reaction gas, abbreviated as U-sessions), the average sensitivity measured for a 40  $\mu$ m/10 Hz laser beam on  $^{185}$ Re (measured on NIST-612) varied between ca. 5.7 and 10.3 kcps ppm $^{-1}$ . For the Adelaide sessions (with variable reaction gas mixtures, abbreviated as Asessions), the average sensitivity for a 50  $\mu$ m/10 Hz spot ablation on  $^{185}$ Re (measured on NIST-610) was 9.1 kcps ppm $^{-1}$  for Asession 1 ( $CH_4 + H_2 + He$ ), 7.3 kcps ppm $^{-1}$  for Asession 2a ( $N_2O$ ), and 6.3 kcps ppm $^{-1}$  for Asession 2b ( $N_2O + He$ ). While the  $CH_4$ -method (U-sessions and Asession 1) produced the highest sensitivity, it also induced the highest Re interference with ca. 0.5% (average USGS) and ca. 0.6% (average Adelaide) Re

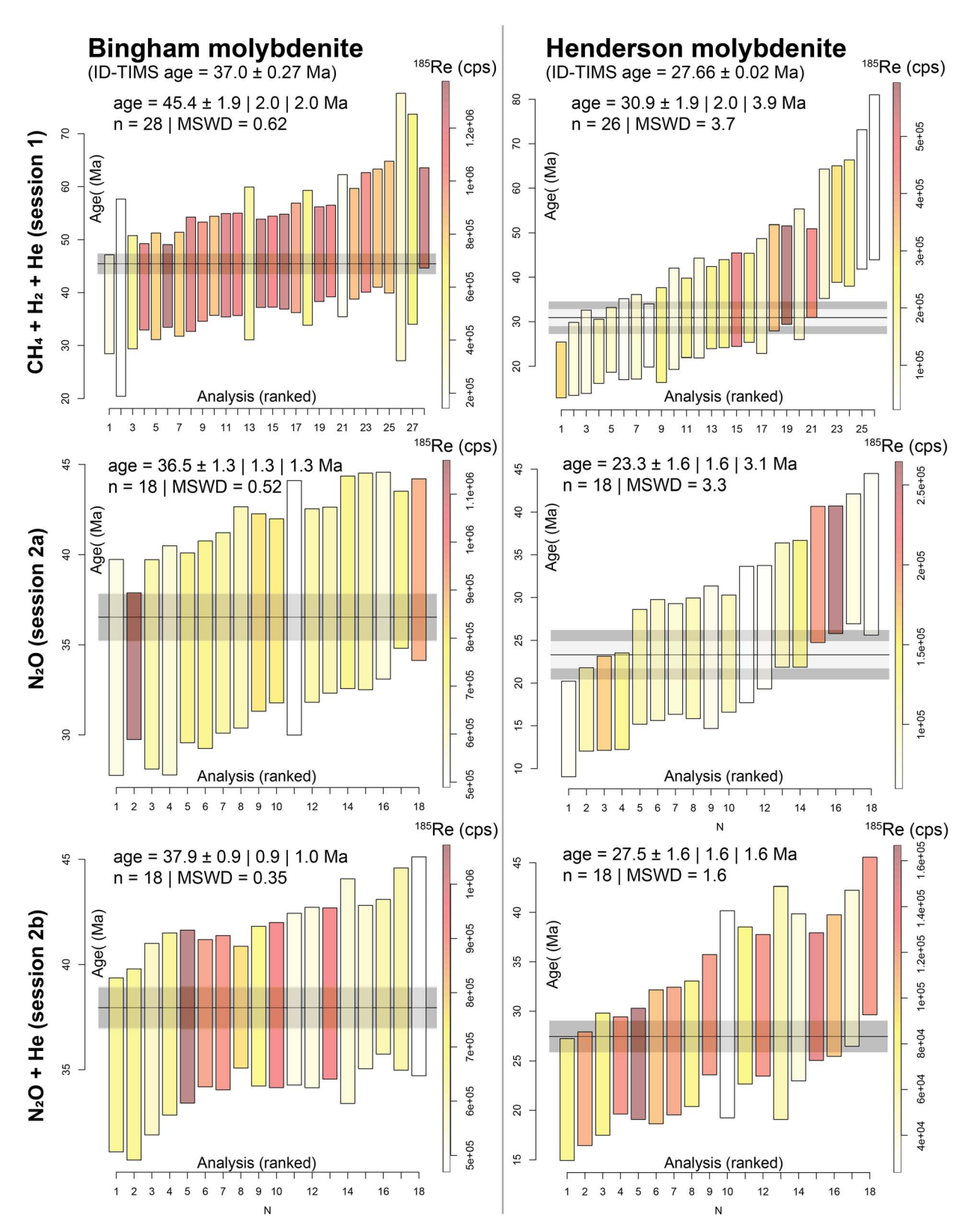


Fig. 1 In situ Re-Os dates for the Bingham and Henderson molybdenite, analysed at Adelaide Microscopy, calculated as weighted means in IsoplotR.<sup>14</sup> Analyses are ranked by age, plotted with 2 SEM uncertainties, and colour coded to <sup>185</sup>Re count rate (cps). Reported weighted mean age uncertainties are 95% confidence intervals, without overdispersion, with overdispersion and with added uncertainty on the decay constant. MSWD = mean squared weighted deviation on the weighted mean Re-Os date.

**JAAS** 

reacting to form ReCH<sub>2</sub><sup>+</sup> (Table 2). This is ca. 45-65% lower compared to previously reported Re reaction rates in absence of H<sub>2</sub> in the reaction cell.<sup>6,7</sup> For the N<sub>2</sub>O method, ca. 0.17% Re reacts to the equivalent ReO<sub>4</sub><sup>+</sup> reaction product (A-session 2a), which is further reduced to 0.02% with added He (5 ml min-1; Asession 2b). Hence, although count rates are compromised, the N<sub>2</sub>O + He method requires a much smaller <sup>187+x</sup>Re interference correction on <sup>187+x</sup>Os. For example, on the secondary reference molybdenite (M252), the interference correction requires removal of 28% Re from Os on mass 187 + 14 amu in A-session 1. 10% on mass 187 + 64 amu for A-session 2a and 3% on mass 187 + 64 amu for A-session 2b (Table 2). Applied to the Cenozoic molybdenite samples, which are much younger and thus have considerably less radiogenic <sup>187</sup>Os ingrowth compared to the Mesoproterozoic M252 molybdenite, the interference correction

accounts for ca. 87-97% in the U-Sessions, 93-95% in A-session 1, 83-87% in A-session 2a and 49-58% in A-session 2b.

#### Cenozoic molybdenite Re-Os dates

The extensive interference subtraction significantly affects the accuracy and precision (as a function of count rate statistics and age dispersion) of the in situ Re-Os dates (Table 2 and Fig. 1). When  $CH_4 + H_2 + He$  is used in the reaction cell (A-session 1, all U-sessions), the Re-Os dates for the Henderson molybdenites are consistently over-dispersed (MSWD between 1.7 and 6.9) and at least for one analytical session (U5), the resulting weighted mean Re-Os date is too young (20.1  $\pm$  5.6 Ma) compared to the IDTIMS reference age (27.66  $\pm$  0.02 Ma; Fig. 1, 2 and Table 2). For the Bingham molybdenites, the CH<sub>4</sub> + H<sub>2</sub> + He method in Adelaide (A-session 1) produced an inaccurate

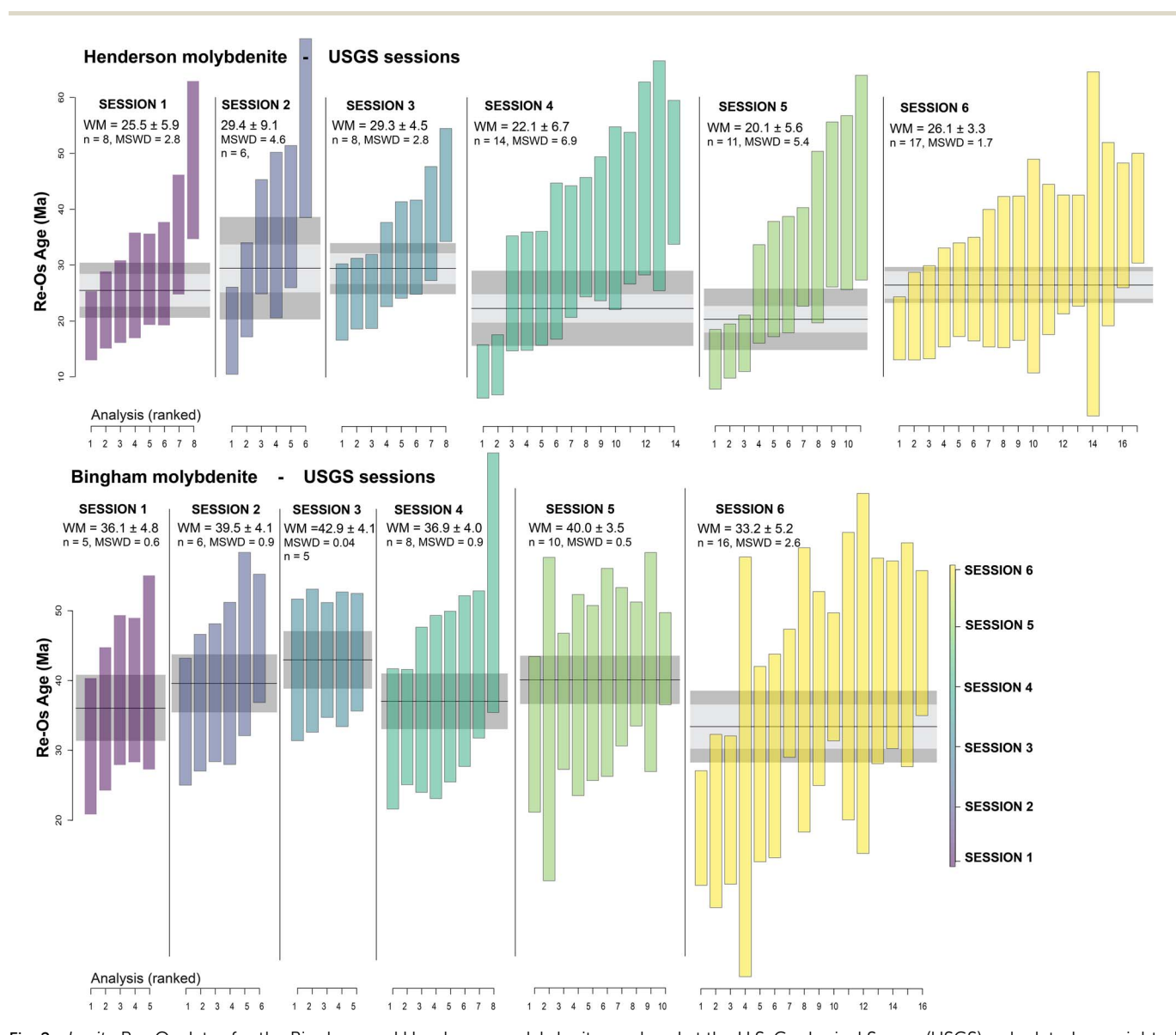


Fig. 2 In situ Re-Os dates for the Bingham and Henderson molybdenite, analysed at the U.S. Geological Survey (USGS), calculated as weighted means in IsoplotR.<sup>14</sup> Analyses are ranked by age and plotted with 2 SEM uncertainties. The resulting Re-Os age uncertainties are 95% confidence intervals including overdispersion (other uncertainties are shown in Tables 1 and 2). MSWD = mean squared weighted deviation on the weighted mean Re-Os date.

Paper

date of 45.4  $\pm$  2.0 Ma, compared to the IDTIMS reference age of  $37.0 \pm 0.3$  Ma (Fig. 1 and Table 2). Furthermore, precision is compromised with the CH<sub>4</sub> + H<sub>2</sub> + He method, producing fully propagated age uncertainties up to 13% in Adelaide and as high as 31% at the USGS. Age precision and accuracy is improved with the N<sub>2</sub>O reaction gas (A-session 2a), producing dates of  $36.5 \pm 1.3$  Ma for Bingham (in agreement with reference age) and 23.3  $\pm$  3.1 Ma for Henderson (younger than reference age). Age dispersion remains large for Henderson with an MSWD of 3.3. For A-session 2b, where He is added to N<sub>2</sub>O in the reaction cell, both molybdenite dates are accurate and at the highest precision: 37.9  $\pm$  1.0 Ma (2.6% uncertainty) for Bingham and  $27.5 \pm 1.6$  Ma (5.8% uncertainty) for Henderson. For both samples, the dataset statistically constitutes a single age population (MSWD = 0.35 for Bingham and 1.6 for Henderson). For the  $N_2O$   $\pm$  He sessions, the background and interference subtracted count rates on  $^{187+64}$ Os are  $\leq 50$  cps for the Henderson molybdenite, approaching the limits of the analytical method, while still producing accurate and precise dates.

# Discussion

#### Interference correction in function of reaction rate and age

While it's important to maximize sensitivity (total count rates), the magnitude of the interference correction of  $^{187+x}$ Re on  $^{187+x}$ Os exerts a dominant control on the accuracy of *in situ* Re–

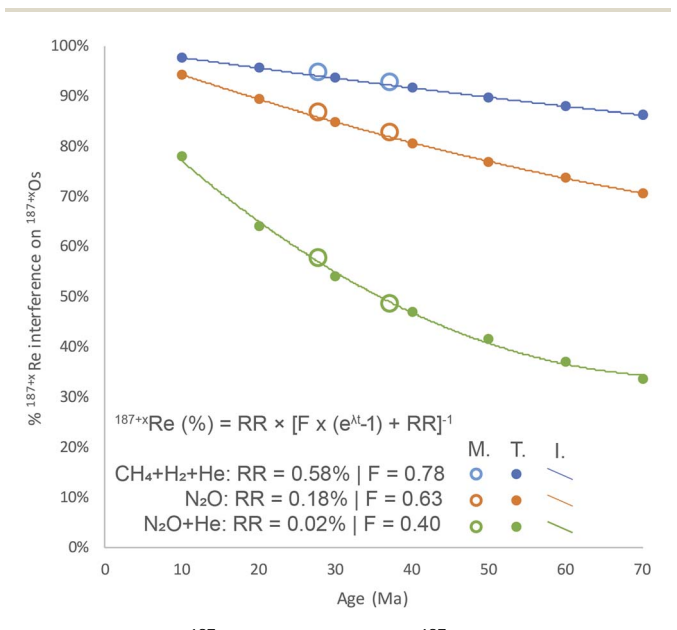


Fig. 3 Percentage  $^{187+x}$ Re interference on  $^{187+x}$ Os plotted as a function of age for the three Adelaide analytical sessions with different reaction gas mixtures. Open symbols represent measured interference percentages (M.), while filled symbols were theorized (T.) based on a theorical formula from ref. 7. The curves are second-order interpolation polynomials (I.) for the theorized values. RR refers to the Re reaction rate (ratio of  $^{185+x}$ Re)/ $^{185}$ Re),  $\lambda$  is the decay constant, t is age in Ma and F is a method-specific  $^{187}$ Os transmission factor. For the CH<sub>4</sub> and N<sub>2</sub>O methods, F was adapted from ref. 7 For the new N<sub>2</sub>O + He method, F was calculated as the ratio between measured and predicted interference curves. This plot can be used to predict the interference percentage based on age and method-specific constants (RR and F).

Os age results, especially for young samples. Hence, an ability to predict the percentage interference would be an important screening tool prior to Re-Os analysis, increasing the likelihood of useful age calculations. Simpson et al.7 determined the interference as a function of Re reaction rate and age: 187+xRe  $(\%) = RR \times [F \times (e^{\lambda t} - 1) + RR]^{-1}$ . Given RR (= Re reaction rate) and F (=<sup>187</sup>Os transmission factor) are reaction-gas specific constants that should be largely invariable once determined for given mass-spectrometer tuning conditions, the interference correction can be predicted in function of age (Fig. 3). For Palaeogene (ca. 66-23 Ma) molybdenite, the interference is predicted to vary between ca. 87% and 95% for the  $CH_4 + H_2 +$ He reaction gas and between ca. 72% and 88% for the N2O reaction gas. Unless very high count rates can be measured (Rerich molybdenite), such large correction will lead to overdispersed and likely inaccurate dates, assuming that the samples are internally homogenous in terms of Re-Os ratios. For the  $N_2O$  + He method, the interference correction remains significant (ca. 35-60%) but we demonstrate accurate and robust dates can be obtained with this approach.

#### Limitations and advantages of in situ Re-Os geochronology

Compared to the conventional ID-TIMS approach, higher sensitivity is required to enable accurate age determination by LA-ICP-MS/MS for young molybdenites. Therefore, Re concentrations need to be sufficiently high ( $^{185}$ Re >100k cps) before attempting *in situ* Re–Os analysis. As demonstrated, an optimized gas mixture is crucial to minimize interference from  $^{187+x}$ Re on  $^{187+x}$ Os, with the N<sub>2</sub>O + He reaction gas being most promising. However, for older (Precambrian) molybdenites, Simpson *et al.*<sup>7</sup> demonstrated fewer differences in obtainable age precision comparing reaction gasses, with the CH<sub>4</sub> method potentially giving better precision for >1 Ga molybdenites. Thus, different reaction gas mixtures should be evaluated as some cater better for old *versus* young molybdenite samples.

In contrast to ID-TIMS, which relies on bulk sample dissolution methods, the *in situ* method is a micro-sampling technique that has the ability to evaluate potential age zonation and/or isotopic disturbance (heterogeneity) across crystals. While age heterogeneity was not observed in the samples for this study (within the obtainable precision of a single analysis), the *in situ* technique is suitable for homogeneity assessments. Isotopic decoupling has been described previously<sup>3,17</sup> but was not observed within the resolution of our analyses.

However, the most important advantage of the *in situ* method is the speed of analysis, where up to 1000 single spot dates can be obtained within a single (*ca.* 24 hours) analytical session. This opens a new window of opportunities for mineral exploration (*e.g.* ref. 18) that can now be extended to young (Palaeogene) molybdenite systems when Re concentrations are sufficiently high.

# Conclusions

We evaluated three reaction gas mixtures for *in situ* (LA-ICP-MS/MS) Re-Os geochronology of young (Cenozoic) molybdenites

JAAS Paper

and demonstrate that  $N_2O$  (0.3 ml min<sup>-1</sup>) + He (5 ml min<sup>-1</sup>) is the optimal reaction gas mixture to sufficiently reduce the isobaric interference of Re onto Os (*ca.* 0.02% Re reaction rate). Robust Re–Os dates were obtained for the Re-rich Palaeogene Bingham Canyon and Henderson molybdenite, validating the approach.

# Data availability

All isotope ratio data and meta-data (reference materials, instrument conditions) are provided in the ESI† and ref. 10.

# **Author contributions**

S. Gl. J. T., S. E. G.: method development, analysis, data interpretation, writing, review and editing. A. K. S.: data interpretation, writing, review and editing.

## Conflicts of interest

There are no conflicts to declare.

# Acknowledgements

S. Gl. was supported by an Australian Research Council Future Fellowship (FT210100906). Jarred Lloyd is thanked for assistance with script writing for uncertainty calculations. JMT and AKS are supported by the U.S. Geological Survey Mineral Resources Program 'From Outcrop to Ions' project (RK00V44). William (Bill) Benzel is thanked for the sample of the Henderson Mine molybdenite. Any use of trade, firm, or product names is for descriptive purposes only and does not imply endorsement by the U.S. Government. Two anonymous reviewers are thanked for their reviews.

## References

1 N. J. Saintilan, D. Selby, R. A. Creaser and S. Dewaele, *Sci. Rep.*, 2018, 8, 14946.

- 2 A. J. Finlay, D. Selby and M. J. Osborne, *Geology*, 2011, 39, 475–478.
- 3 D. Selby and R. A. Creaser, *Geochim. Cosmochim. Acta*, 2004, 68, 3897–3908.
- 4 H. J. Stein, R. J. Markey, J. W. Morgan, J. L. Hannah and A. Scherstén, *Terra Nova*, 2001, 13, 479–486.
- 5 K. J. Hogmalm, I. Dahlgren, I. Fridolfsson and T. Zack, *Miner. Deposita*, 2019, **54**, 821–828.
- 6 R. Tamblyn, S. Gilbert, S. Glorie, C. Spandler, A. Simpson, M. Hand, D. Hasterok, B. Ware and S. Tessalina, *Geostand. Geoanal. Res.*, 2024, 48, 393–410.
- 7 A. Simpson, S. Glorie, S. Gilbert, R. Tamblyn and M. G. Gadd, *Chem. Geol.*, 2024, **670**, 122384.
- 8 J. T. Chesley and J. Ruiz, in *Geology and Ore Deposits of the Oquirrh and Wasatch Mountains*, Society of Economic Geologists, Utah, 1998, vol. 29.
- 9 R. Markey, H. J. Stein, J. L. Hannah, A. Zimmerman, D. Selby and R. A. Creaser, *Chem. Geol.*, 2007, 244, 74–87.
- 10 J. M. Thompson and A. K. Souders, Re-Os Geochronology of Molybdenite and Metalliferous Black Shales, U.S. Geological Survey Data Release, 2025, DOI: 10.5066/P13ZTY3I.
- 11 J. W. Gramlich, T. J. Murphy, E. L. Garner and W. R. Shields, J. Res. Natl. Bur. Stand., Sect. A, 1973, 77, 691–698.
- 12 K. Suzuki, L. Qi, H. Shimizu and A. Masuda, *Geochim. Cosmochim. Acta*, 1993, 57, 1625–1628.
- 13 A. Norris and L. Danyushevsky, *Towards estimating the* complete uncertainty budget of quantified results measured by LA-ICP-MS, Goldschmidt, Boston, 2018.
- 14 P. Vermeesch, Geosci. Front., 2018, 9, 1479-1493.
- 15 S. Gilbert, L. Danyushevsky, P. Robinson, C. Wohlgemuth-Ueberwasser, N. Pearson, D. Savard, M. Norman and J. Hanley, *Geostand. Geoanal. Res.*, 2013, 37, 51–64.
- 16 J. Völkening, T. Walczyk and K. G. Heumann, Int. J. Mass Spectrom. Ion Processes, 1991, 105, 147–159.
- 17 H. Stein, A. Scherstén, J. Hannah and R. Markey, *Geochim. Cosmochim. Acta*, 2003, **67**, 3673–3686.
- 18 A. Simpson, S. Glorie, M. Hand, S. E. Gilbert, C. Spandler, M. Dmitrijeva, G. Swain, A. Nixon, J. Mulder and C. Münker, Geosci. Front., 2024, 15, 101867.